THE ASTROPHYSICAL JOURNAL, 276:211–220, 1984 January 1

METHYL ACETYLENE AS A TEMPERATURE PROBE FOR DENSE INTERSTELLAR CLOUDS

T. B. H. KUIPER, E. N. RODRIGUEZ KUIPER,[1] AND DALE F. DICKINSON[2]
Jet Propulsion Laboratory, California Institute of Technology

B. E. TURNER
National Radio Astronomy Observatory

AND

B. ZUCKERMAN
Department of Physics and Astronomy, University of Maryland
Received 1980 September 22; accepted 1982 December 13

ABSTRACT

Methyl acetylene (propyne) appears to be a convenient and reliable probe of kinetic temperature for dense ($\gtrsim$few $\times 10^4$ cm^{-3}) molecular clouds. A method is presented for fitting a $(J+1)-J$ K-multiplet to obtain the kinetic temperature from a single observation, facilitating the direct construction of kinetic temperature maps. Observations of Tau MC1, Ori MC1, Sgr B2, DR 21, DR 21 (OH), and S140 are presented to demonstrate the validity of the technique. Determination of methyl acetylene column densities requires, in addition, knowledge of the rotational excitation temperature. The relative abundance of CH_3CCH appears to be within a factor of 2 of 2.5×10^{-9}. Because of the large uncertainties in estimates of total gas column density, it is not clear whether there is genuine source-to-source variation in the CH_3CCH relative abundance.

Subject headings: interstellar: molecules — nebulae: general

I. INTRODUCTION

Methyl acetylene (CH_3C_2H) was first detected in the Galactic Center by Snyder and Buhl (1973). One line ($J_K = 5_0$–4_0) has been reported in Orion (Lovas *et al.* 1976). This molecule has considerable significance as a tracer of two common chemical groups and demonstrable potential as a temperature probe of molecular clouds. One technique for exploiting the latter aspect, which requires observation of two multiplets with significant separation in J, has been presented by Hollis *et al.* (1981).

Because the rotational energy levels of a symmetric top molecule are given by $E = hBJ(J+1) + h(A-B)K^2$, where A and B are the usual rotational constants (Herzberg 1945), methyl acetylene has the energy level structure shown in Figure 1. Radiative transitions between the K-ladders are forbidden by the radiative selection rules ($\Delta J = 0, \pm 1$, $\Delta K = 0$), so that the relative populations of the K-ladders depend primarily on the kinetic temperature of the colliding particles. Because the energy separation of the levels is small, the absence of the $J < K$ levels for the higher ladders will have only a minor influence on the relative populations in the higher levels of the ladders as long as the rotational excitation (i.e., collision rate) for the K-ladders is not very small. If we assume a collision diameter of $\sim$10 Å, we find that densities a few times 10^4 cm^{-3} are sufficient to maintain reasonable populations in the $J = 6$ levels even at low temperatures ($\gtrsim$20 K). By implication, the low K-ladders ($K = 0, 1, 2$) may for many molecular clouds be treated as having identical population distributions in the higher J levels. A determination of the ratios of the populations of these higher J transitions is then a measure of the relative total populations of the ladders and, hence, of kinetic temperature.

The simultaneous observation of all the members of a multiplet eliminates many calibration problems. Since the dipole moment is only 0.78D (Bauer *et al.* 1979), CH_3C_2H is more easily thermalized than other symmetric rotors (such as CH_3CN with 3.9D). This suggests that line intensity data may be analyzed assuming LTE, so that the kinetic temperature may be derived. Further, the relatively weak intensities observed in interstellar clouds suggest that the simplifying assumption of low optical depth may be valid. This paper explores the potential of CH_3C_2H as a convenient temperature indicator.

II. OBSERVATIONS

Observations of the $J = 6$–5 multiplet of CH_3C_2H were made in 1975 February and 1981 January and of the $J = 5$–4 and 6–5 multiplets in 1981 January with the NRAO[3] 11 m paraboloid at Kitt Peak, Arizona. The source parameters are given in Table 1. The receiver was an 80–120 GHz cooled mixer; spectral resolution was provided by a 256 channel spectrometer with 30, 100, 250, and 500 kHz filters. The 100 and 250 kHz filters proved the most useful. Single-sideband system temperature was approximately 800 K in 1975 and 500 K in 1981.

[1] Ball Aerospace Systems Division employee under contract to JPL.
[2] NAS-NRC Senior Resident Research Associate.
[3] NRAO is operated by Associated Universities, Inc. under contract to the National Science Foundation.

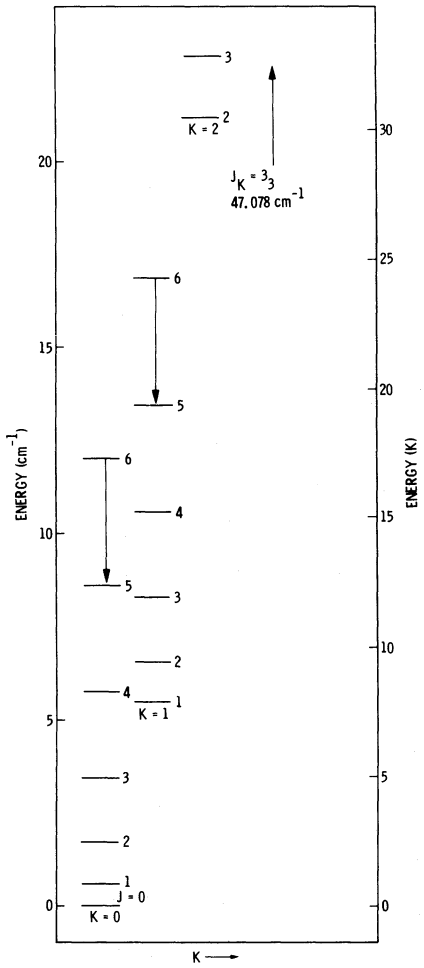

FIG. 1.—The methyl acetylene rotational energy levels

III. ANALYSIS OF THE OBSERVATIONS

Assuming the optical depth for a rotational transition can be written as

$$\tau = \frac{8\pi^3}{3h}\,\mu^2 S_{ul}\, N \frac{g_K g_I}{Q_r} \exp\left(-\frac{E_l}{kT}\right)\left[1 - \exp\left(-\frac{h\nu_{lu}}{kT}\right)\right]\phi'(V)\,, \tag{1}$$

where μ is the dipole moment, S_{ul} is the line strength (u and l designating the upper and lower states of the transition), N is the column density, and $\phi'(V)$ is the line shape as a function of velocity. The K degeneracy, g_K, for a symmetric top reflects the fact that K and $-K$ are indistinguishable:

$$g_K = 1 \qquad K = 0\,,$$
$$= 2 \qquad K \neq 0\,.$$

The reduced (i.e., divided by $[2I + 1]^3$) nuclear spin statistical weight (for $I = \frac{1}{2}$) is

$$g_I = \tfrac{1}{2} \qquad K = 0, 3, 6, 9, \ldots$$
$$g_I = \tfrac{1}{4} \qquad K \neq 0, 3, 6, 9, \ldots\,.$$

The LTE partition function is given by Herzberg (1945) as

$$Q_r = \frac{5.34 \times 10^6}{\sigma}\left[\frac{T^3}{B^2 A}\right]^{1/2} \tag{2}$$
$$= 0.523 T^{3/2} \text{ for methyl acetylene}\,,$$

TABLE 1

SUMMARY OF OBSERVATIONS

Source	R.A. (1950)	Decl. (1950)	J'–J	$T_A^*(K=0)$[a] (K)	V_{LSR} (km s^{-1})	ΔV (km s)	Filter Resolution (kHz)
W3 SR	$2^h21^m54^s9$	61°51′51″	5–4	<0.2	...	...	...
W3 OH	2 23 16.7	61 38 54	6–5	<0.3	...	...	...
Tau MC1(a)	4 38 41.9	25 35 45	5–4	0.94 ± 0.19	5.8 ± 0.02	0.4 ± 0.05	30
			6–5	0.57 ± 0.10	5.8 ± 0.1	0.5 ± 0.1	30
Tau MC1(b)	4 38 41.9	25 33 45	5–4	0.67 ± 0.17	5.7 ± 0.03	0.5 ± 0.08	30
			6–5	0.59 ± 0.16	5.9 ± 0.03	0.9 ± 0.2	100
Ori MC1	5 32 47.0	−5 24 24	5–4	0.33 ± 0.07	9.2 ± 0.2	3.6 ± 0.4	250
			6–5	0.40 ± 0.06	9.6 ± 0.2	3.2 ± 0.3	500
NGC 2264	6 38 28.4	9 32 12	5–4	0.14 ± 0.04	7.3 ± 0.2	1.7 ± 0.4	250
			6–5	<0.20	...	...	...
IRC +10216	9 45 14.8	13 30 40	5–4	<0.1	...	...	...
			6–5	<0.1	...	...	...
L134	15 51 00.0	−4 26 58	5–4	<0.35	...	...	...
			6–5	<0.60	...	...	...
L183	15 51 34.0	−2 43 31	5–4	<0.25	...	...	...
ρ Oph	16 23 15.0	−24 19 00	6–5	<0.40	...	...	...
Sgr B2	17 44 11.0	−28 22 30	5–4	0.90 ± 0.11	60.2 ± 0.4	19.3 ± 1.0	250
			6–5	0.69 ± 0.05	59.3 ± 0.3	17.3 ± 0.6	500
W51	19 21 27.0	14 24 30	5–4	0.40 ± 0.14	59.0 ± 1.6	6.8 ± 3.1	250
			6–5	0.26 ± 0.09	56.5 ± 0.7	7.4 ± 1.9	500
DR 21	20 37 13.9	42 09 00	6–5	0.29 ± 0.07	−2.2 ± 0.3	3.3 ± 0.5	500
			6–5	0.33 ± 0.09	−2.0 ± 0.2	2.3 ± 0.4	250
DR 21(OH)	20 37 14.0	42 12 00	6–5	0.30 ± 0.07	−3.7 ± 0.2	3.0 ± 0.5	500
			6–5	0.32 ± 0.04	−3.3 ± 0.2	3.3 ± 0.3	500
S140	22 17 40.9	63 03 45	6–5	0.37 ± 0.07	−7.1 ± 0.1	2.9 ± 0.3	250
Cep A	22 54 26.5	61 44 37	5–4	<0.20	...	...	...
			6–5	<0.15	...	...	...

[a] The quoted error is the rms noise in the baseline. The upper limits are 3 times the rms noise.

where A and B are the rotational constants (= 158590 and 8546 MHz, respectively), and $\sigma = 3$ reflects the symmetry of the methyl group. The dipole moment is $0.78D$, and the line strength is

$$S_{J,K\to J+1,K} = \frac{(J+1)^2 - K^2}{J+1}.$$

If we assume a Gaussian line shape

$$\phi'(V) = \frac{2\sqrt{\ln 2}}{W\sqrt{\pi}} \exp\left[-4\ln 2\left(\frac{V}{W}\right)^2\right],$$

where W is the velocity full width at half-maximum in km s^{-1}, then

$$\tau = \frac{1.34\times 10^{-8}}{T^{3/2}}(S_{ul}\,g_K\,g_I)N \exp\left(-\frac{E_l}{kT}\right)\left[1-\exp\left(-\frac{h\nu_{lu}}{kT}\right)\right]\phi'(V),$$

and assuming $\tau \ll 1$, the brightness temperature,

$$T_B = \tau T = \frac{1.26\times 10^{-13}}{T^{1/2}}(S_{ul}\,g_K\,g_I)\left(\frac{N}{W}\right)\exp\left(-\frac{E_l}{kT}\right)\left[1-\exp\left(-\frac{h\nu_{lu}}{kT}\right)\right]\exp\left[-2.773\left(\frac{V}{W}\right)^2\right]$$

for V and W in km s^{-1}, and N in cm^{-2}. For a multiplet of lines, we may write:

$$T_B = 1.26\times 10^{-13}\left(\frac{N}{W}\right)\left\{\frac{1-\exp\left[-(h\nu_{lu}/kT)\right]}{T^{1/2}}\right\}\sum_{K=0}^{J}(g_I\,g_K\,S_{lu})_K \exp\left(-\frac{1.44E_{JK}}{T}\right)\exp\left[-2.773\left(\frac{V-V_0-\Delta V_K}{W}\right)^2\right]$$

where V_0 is the LSR velocity, ΔV_K is the velocity offset of the Kth component relative to the $K=0$ component, and ν_{lu}, the line rest frequency, is to sufficient accuracy the same for all lines in the multiplet. We use ν_{lu} for $K=0$. E_{JK} ($\equiv E_l$) is in units of cm^{-1}. Parameters are given in Table 2. Thus we have

$$T_B = N * F(T) * \frac{1}{W}\sum_{K=0}^{J} f_K(T)\exp\left[-2.773\left(\frac{V-V_0-\Delta V_K}{W}\right)^2\right], \tag{3a}$$

TABLE 2

MOLECULAR CONSTANTS FOR OBSERVED MULTIPLETS

ν(MHz)	K	E_{JK} (cm^{-1})	ΔV_K (km s^{-1})	S	$g_K g_I S$
		$J = 5$–4			
85431.224	4	83.303	91.455	1.8	0.9
85442.528	3	49.358	51.766	3.2	3.2
85450.730	2	25.106	22.969	4.2	2.1
85455.622	1	10.553	5.79	4.8	2.4
85457.272	0	5.701	0.0	5.0	2.5
		$J = 6$–5			
102499.110	5	129.781	143.20	1.83	0.92
102516.573	4	86.153	92.03	3.33	1.67
102530.348	3	52.209	51.67	4.5	4.5
102540.144	2	27.957	22.97	5.33	2.67
102546.024	1	13.403	5.74	5.83	2.92
102547.984	0	8.552	0.0	6.0	3.0

$$F(T) = 1.26 \times 10^{-13}\left[1 - \exp\left(-\frac{4.783 \times 10^{-5}\nu_{lu}}{T}\right)\right]\Big/ T^{1/2}\,, \tag{3b}$$

$$f_K(T) = (g_I g_K S_{ul})_K \exp\left(-\frac{1.44E_{JK}}{T}\right), \tag{3c}$$

where ν_{lu} is in MHz. We fit the observations to this function (program CHIFIT from Bevington 1969) to derive N, T, W, and V_0.

We consider now how the derived temperature T differs from the kinetic temperature of the gas when the K-ladders are not in thermodynamic equilibrium. Following Hollis *et al.* (1981), we adopt a two-temperature model in which T_R describes the excitation of the K-ladders and T_K describes the relative populations of the metastable ($J = K$) levels. The lower energy level can be expressed as

$$E_{JK} = [h(A - B)K^2 + hBK(K + 1)] + [hBJ(J + 1) - hBK(K + 1)]\,,$$

where the first term in square brackets is the energy of the metastable level of a K-ladder, and the second term is the energy by which E_{JK} lies above the metastable level. We then write equation (3c) as

$$f_K(T_R, T_K) = (g_I g_K s_{ul})_K \exp\left[-\frac{h(A - B)K^2 + hBK(K + 1)}{kT_K} - \frac{hBJ(J + 1) - hBK(K + 1)}{kT_R}\right].$$

We also note that equation (3b) is a function of T_R alone, since it involves two levels in the same ladder. Since the sum in equation (3a) is over K, we may rewrite this as

$$T_B = \frac{NF(T_R)}{W}\exp\left(-\frac{hBJ(J + 1)}{kT_R}\right)\sum_{K=0}^{J}(g_I g_K S_{ul})_K \exp\left[-\frac{h(A - B)K^2}{kT_K}\right] * \exp\left[-\frac{hBK(K + 1)}{k}\left(\frac{1}{T_K} - \frac{1}{T_R}\right)\right]\exp\left[-2.773\left(\frac{V - V_0 - \Delta V_K}{W}\right)^2\right]. \tag{4}$$

We see that in the case of LTE, the temperature is determined from the terms

$$\exp\left[-\frac{h(A - B)K^2}{kT}\right],$$

whereas in a two-temperature model, this term is replaced by

$$\exp\left[-\frac{h(A - B)K^2}{kT_K}\right]\exp\left[-\frac{hBK(K + 1)}{K}\left(\frac{1}{T_K} - \frac{1}{T_R}\right)\right].$$

Equating these, we can express the apparent T derived from the fit as a function of T_K and T_R:

$$\frac{T_K}{T} = 1 + \frac{BK(K + 1)}{(A - B)K^2}\left(1 - \frac{T_K}{T_R}\right). \tag{5}$$

Since $B \ll A$, the ratio T_K/T_R may depart considerably from unity without having much effect on T_K/T. Figure 2 shows a plot of equation (5). In general, if $T_R > T_K/2$ the effect of assuming LTE is negligible.

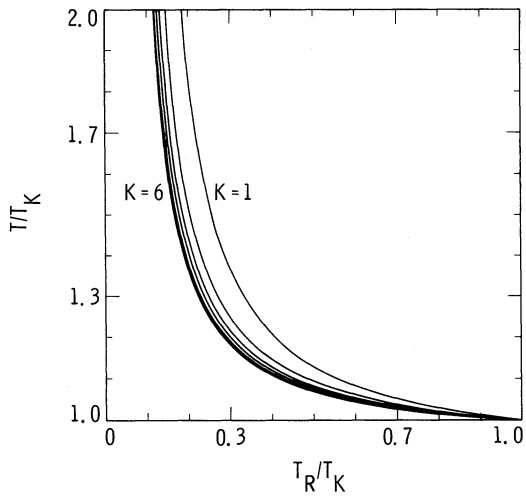

FIG. 2.—Plot of the ratio of the apparent kinetic temperature to the true kinetic temperature as a function of the ratio of the rotational temperature to the kinetic temperature according to eq. (7).

The effect of the approximation on evaluating the column density is more serious. We recognize that in the limit of $h\nu_{lu} \ll kT$, which is applicable in this case, equation (3b) is, except for some constants, essentially the inverse of the partition function is given by

$$Q = \sum_{K=0}^{\infty} (g_I g_K)_K \exp\left[-\frac{h(A-B)K^2}{kT_K}\right] \exp\left[-\frac{hBK(K+1)}{K}\left(\frac{1}{T_K}-\frac{1}{T_R}\right)\right] * \sum_{J=K}^{\infty}(2J+1)\left[\exp-\frac{hBJ(J+1)}{kT_R}\right].$$

Since $hB \ll kT$, we can replace the sums with integrals; using the substitution $x = J(J+1)$,

$$\sum_{J=K}^{\infty}(2J+1)e^{-hBJ(J+1)/kT_R} = \int_{K^2}^{\infty} dx e^{-hBx/kT_R}$$

$$= \frac{kT_R}{hB} e^{-hBK^2/kT_R}. \tag{6}$$

We have started the integral halfway between $(K-1)K$ and $K(K+1)$ which is the beginning of the interval centered at $K(K+1)$. Thus,

$$Q = \frac{kT_R}{hB}\sum_{K=0}^{\infty}(g_I g_K)_K \exp\left(-\frac{hAK^2}{kT_K}\right)\exp\left[-\frac{hBK}{k}\left(\frac{1}{T_K}-\frac{1}{T_R}\right)\right].$$

Therefore, each term in the K-sum in the partition function will have to be multiplied by a correction of the form

$$\frac{T_R}{T}\exp\left[-\frac{hBK}{kT_K}\left(\frac{T_K}{T_R}-1\right)\right].$$

Since $hB \ll kT_K$, the exponential term has an effect only at large K, but multiplies summation terms which decrease in importance with K^2. The principal effect, therefore, is to modify the dominant $K = 0$ term, and hence the partition function, by T_R/T. The correction factor to be applied to the apparent column density, assuming $T_K \approx T$, is therefore

$$\frac{T_R}{T}\exp\left[-\frac{hBJ(J+1)}{k}\left(\frac{1}{T}-\frac{1}{T_R}\right)\right]. \tag{7}$$

It is of interest to consider the consequence of having two regions along the line of sight with different kinetic temperatures. If the regions have significantly different line widths or velocities with respect to the local standard of rest, this will be apparent in a plot of the residuals of the fit. In that case, equation (3) can be extended to include the second region in the fit, the model then having eight parameters instead of four. When the line widths and LSR velocities of the two regions are similar, however, the temperature and density by a single region model will be affected by the unavoidable averaging. To study this effect, we carried out the fitting procedure on synthetic spectra formed by adding T_B (from eq. [3]) for a hot region (50, 100, and 200 K, respectively) to T_B for a cool (20 K) region. The ratio of the column densities for the two regions was varied and the resulting apparent kinetic temperatures plotted in Figure 3*a*. Because the partition function increases strongly with temperature, the hot region's lines are greatly weakened, and the resulting derived kinetic temperature is strongly dominated by the cool region. In effect, the method tends to be insensitive to the presence of small hot spots in the presence of cool gas.

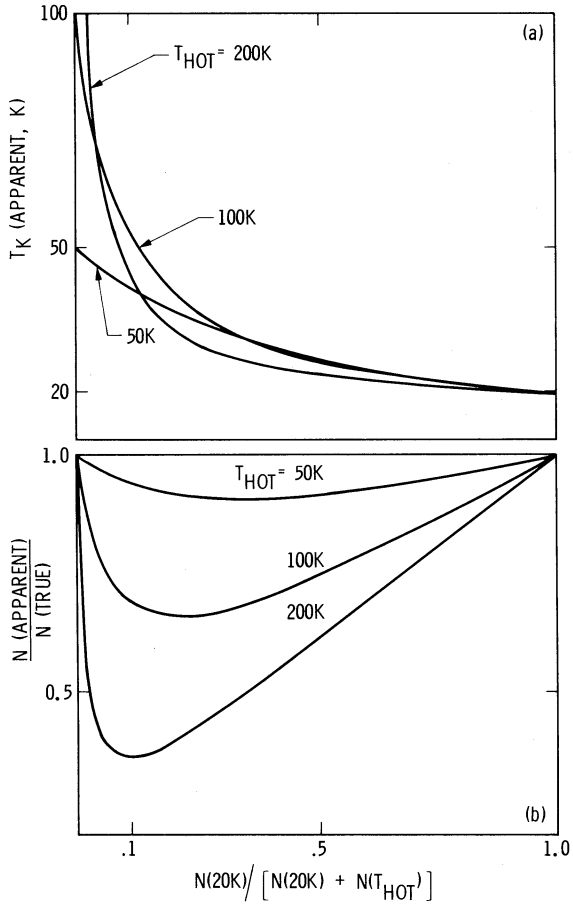

FIG. 3.—The results of fitting synthetic spectra are presented for different relative column densities of hot (50, 100, and 200 K) and cool (20 K) gas. The upper panel (*a*) shows the derived apparent kinetic temperature, and the lower panel (*b*), the ratio of the apparent column density to the actual total (hot and cold gas) column density in the models.

Since the hot gas contributes weakly to the total signal, the column density will be underestimated when hot gas is present. Figure 3*b* shows the ratio of the apparent to the true column density for the two region models which we fitted.

IV. RESULTS

The results of the observations are given in Table 1. The derived parameters are given in Table 3. The uncertainties are one standard deviation derived by the fitting procedure from the noise in the spectra. The uncertainties are generally quite large which is a consequence of the high noise level in the spectra. As the sensitivity of millimeter receivers has increased by a factor of 2 since we made these observations, and continues to improve, the use of this method becomes more practical.

We now discuss the results for the individual sources (except NGC 2264 and W51 for which the data are of low quality).

a) Sgr B2

It is apparent that the observed lines are highly broadened and blended together (Fig. 4), so that it is interesting to see how well equation (3) can be fitted to the data.

Line profiles in the direction of Sgr B2 are complex (e.g., Scoville, Solomon, and Penzias 1975). ^{12}CO, HCN, and CS show peaks at $\sim$50 and $\sim$90 km s^{-1} with a dip between 60 and 70 km s^{-1}. However, less abundant species such as $C^{18}O$, HNCO, OCS, and CH_3CN have a single peak at $\sim$60 km s^{-1} and line widths of $\sim$20 km s^{-1}. Our results (Fig. 4 and Table 1) are consistent with these. The extended molecular cloud at Sgr B2 is believed to have a gas temperature between 20 and 30 K (Scoville, Solomon, and Penzias 1975; Harper 1974). However, CH_3CN shows a distinctly higher excitation temperature, $\sim$100 K (Solomon *et al.* 1973) at the central position in the cloud which we observed. Our observation, which indicates a temperature elevated above that of the extended cloud, is probably due to a blend from a hot core (seen in CH_3CN) and an extended cool cloud (seen in CO, etc.). It will prove interesting to map the source in this line, particularly with higher angular resolution.

Hollis *et al.* (1981) have analyzed $J = 9$–8 observations of methyl acetylene in Sgr B2 in conjunction with our $J = 6$–5 data to obtain both a rotational temperature of 18.9 $\pm$ 1.2 K and a kinetic temperature of 47 $\pm$ 6 K. Thus, from Figure 2 we would

TABLE 3

DERIVED PHYSICAL PARAMETERS

Source	Transition	Apparent Column Density (10^{14} cm^{-2})	Apparent Kinetic Temperature (K)
Tau MC1(a)..	5–4	0.75 ± 0.24	21.5 ± 7.5
		0.49 ± 0.28	20.3 ± 12.5
	6–5	0.33 ± 0.08	21.4 ± 9.0
Tau MC1(b)..	5–4	0.49 ± 0.41	25.7 ± 21.0
	6–5	0.32 ± 0.16	22.6 ± 14.2
Ori MC1	5–4	2.7 ± 0.8	37.3 ± 10.0
	6–5	4.8 ± 1.1	63.1 ± 13.0
NGC 2264....	5–4	0.53 ± 0.29	35.3 ± 18.9
Sgr B2	5–4	30.0 ± 4.2	45.7 ± 5.8
	6–5	20.0 ± 1.6	55.1 ± 3.9
W51.....	5–4	1.7 ± 0.45	10.5 ± 12.7
	6–5	2.5 ± 1.0	32.4 ± 13.5
DR 21	6–5	1.6 ± 0.52	32.1 ± 10.8
		0.84 ± 0.24	21.1 ± 8.2
DR 21(OH)...	6–5	2.8 ± 1.2	53.2 ± 20.0
		1.8 ± 0.36	33.0 ± 6.9
S140	6–5	1.7 ± 0.36	32.1 ± 6.7

expect our derived kinetic temperature to be too large by $\sim 15\%$ and, indeed, our weighted mean value for the two transitions is 52.2 ± 3.2, agreeing with the result of Hollis *et al.* (1981).

If we apply the correction factor (eq. [7]) to the apparent column densities, the corrected column densities are $(1.4 \pm 0.2) \times 10^{15}$ cm^{-2} and $(1.0 \pm 0.1) \times 10^{15}$ cm^{-2} for the $J = 5$–4 and 6–5 transitions, respectively, with a weighted mean of $(1.2 \pm 0.1) \times 10^{15}$ cm^{-2}. The total hydrogen column density in the 50–75 km s^{-1} gas is estimated to be 10^{24} cm^{-2} (Scoville, Solomon, and Penzias 1975), so that the apparent abundance of CH_3C_2H is about 1.2×10^{-9}. The hot gas, which Solomon *et al.* (1973) deduced to be a temperature of ~ 100 K from their CH_3CN analysis may also be subject to the effect which we discussed at the end of § III. Figure 3 shows that the above determination of the CH_3CCH column density therefore underestimates the actual column density by a factor of 1.5 or more, depending on the actual temperatures and densities of the hot and cold gas. We conclude that the relative abundance is $\geq 1.8 \times 10^{-9}$.

b) Orion MC1

Figure 5*a* shows the $J = 6$–5 data, after baseline correction, and the residuals after fitting equation (3). The $K = 0$ and 1 components are clearly visible, and the $K = 2$ and 3 components are seen at a level comparable to the largest noise spike. The $K = 4$ and 5 components are lost in the noise. Nevertheless, the results of fitting equation (3) give parameters for the line width and velocity which are in excellent agreement with parameters obtained from other molecules. For example, $H^{13}CO^+$ $J = 1$–0 has $\Delta V = 3.4 \pm 0.9$ km s^{-1} and $V_{LSR} = 9.2$ km s^{-1} (Snyder *et al.* 1976).

It is surprising that the $J = 6$–5 and $J = 5$–4 transitions give radically different temperatures. The $K = 2$ and 3 features do appear to be weaker in the $J = 5$–4 spectrum (see Fig. 5*b*). This was also observed by Lovas *et al.* (1976). The reason for the unusual behavior of the $J = 5$–4 transition is not clear.

The $J = 6$–5 data yield a temperature consistent with other temperature data for Orion. Pickett and Davis (1979) analyzed

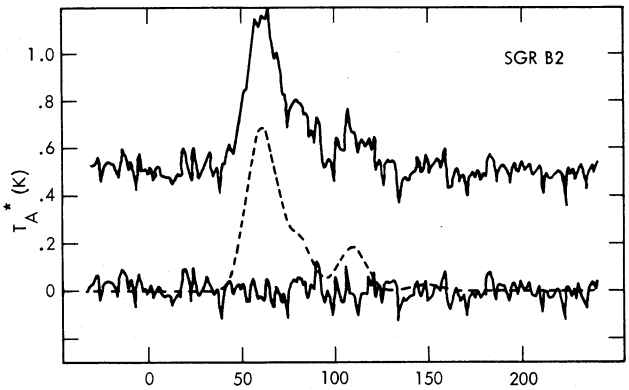

FIG. 4.—The Sgr B2 methyl acetylene $J = 6$–5 spectrum ($\alpha = 17^h44^m11\overset{s}{.}0$, $\delta = -28°22'30''$, 1950). The upper trace shows the original data. The lower trace shows the fitted function and the residuals.

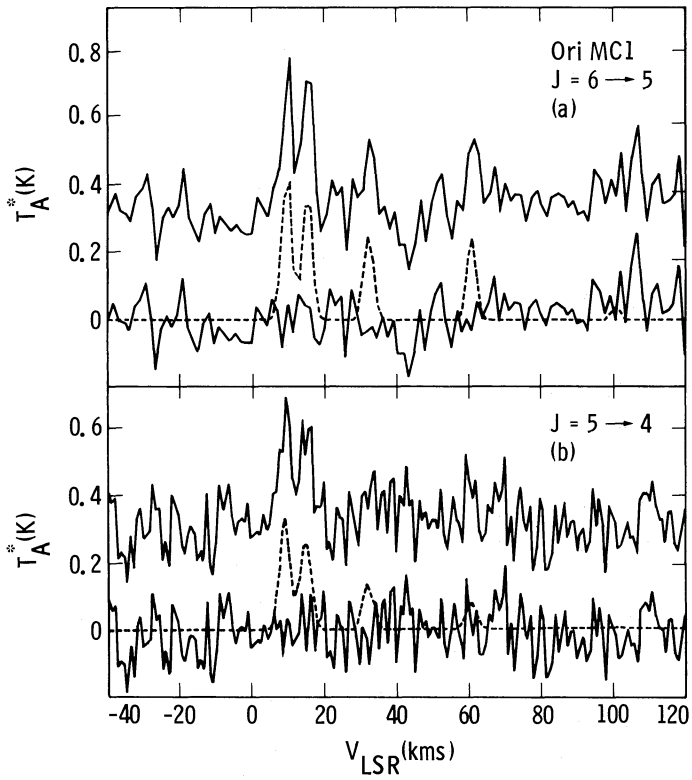

FIG. 5.—Methyl acetylene spectrum in Ori MC1 ($\alpha = 5^h32^m47^s$, $\delta = 5°24'24''$, 1950) with the same format as in Fig. 3. The $J = 6$–5 transition is given in (*a*), and the $J = 5$–4 transition in (*b*). Note the relative weakness of the $K = 2$ and 3 features in the 5–4 spectrum.

the relative intensities of SO_2 transitions and derived a rotational temperature of 68 ± 4 K. The great difference in widths for CH_3C_2H and SO_2 makes it uncertain, however, whether these results can be meaningfully compared. Hollis *et al.* (1983) find that the torsional ground-state transitions of methanol yield a rotational temperature of 89 ± 15 K. CO brightness temperature and IR color temperatures also fall in the range of 80–85 K. Caution is needed in making these comparisons since different indicators may sample different regions of this complex source.

We have no estimate of the rotational excitation temperature, but it is likely to be similar to the kinetic temperature because the density is $\sim 10^5$ cm^{-3} (Evans *et al.* 1975; Linke and Goldsmith 1980). The total hydrogen column density is estimated to be 2×10^{23} cm^{-2} (Evans *et al.* 1975), giving a relative methyl acetylene abundance of 2.4×10^{-9}.

c) Tau MC1

The weighted mean apparent temperature for both Tau MC1 positions is 21.7 ± 4.8 K. Avery, MacLeod, and Broten (1982) modeled this cloud on the basis of HC_3N observations and deduced $T_K = 17$ K for the core region. They estimate the density of this region to be 6×10^4 cm^{-3} which supports our estimate that densities a few times 10^4 cm^{-3} are sufficient to excite the rotational ladders of CH_3CCH.

The mean apparent column density of CH_3CCH is $(3.7 \pm 0.7) \times 10^{13}$ cm^{-3} which is approximately one-third that of HC_3N (Avery, MacLeod, and Broten 1982). The somewhat different values obtained for the $J = 5$–4 and $J = 6$–5 data sets are probably due to calibration uncertainty in the receiver sideband ratio since the Fabry-Perot filter was not used. There is no evident difference in column density at the two positions. Using parameters derived by Avery, MacLeod, and Broten (1982) and assuming a line-of-sight dimension comparable to the dimensions of the cloud core in the plane of the sky, the H_2 column density lies in the range $(0.75\text{–}1.5) \times 10^{22}$ cm^{-2}, giving a CH_3CCH relative abundance of $(2.5\text{–}5) \times 10^{-9}$ which is comparable to that in Orion.

d) DR 21, DR 21 (OH)

Although the observations have a low signal-to-noise ratio, the line widths and velocities are in agreement with those for ^{13}CO (Dickel, Dickel, and Wilson 1978) and in better agreement with those found for CS (Turner *et al.* 1973). The CO corrected antenna temperatures for DR 21 and DR 21 (OH) are 24.5 and 26.4 K, respectively (Dickel, Dickel, and Wilson 1978). If the forward beam coupling efficiency (η_f; Ulich and Haas 1976) were 0.9 (corresponding to a 30′ diameter circular source), the implied CO rotational temperatures would be 27.2 and 29.1 K, respectively. Since the source is smaller, the CO brightness temperatures likely are higher (but the source's irregular shape does not encourage a theoretical calculation of η_f). Cheung (1976) has derived a kinetic temperature of 23 K from NH_3 observations of DR 21 (OH) while Schwartz, Bologna, and Waak

(1978) derived a temperature of 22 ± 4 K for DR 21. If we apply the correction factor derived by Ho, Martin, and Barrett (1981) to these observations, we obtain a kinetic temperature of 33 ± 5 K. Our weighted average apparent kinetic temperature of 30.1 ± 4.6 K is in good agreement with this result.

The weighted mean apparent CH_3CCH column density is $(1.0 \pm 0.2) \times 10^{14}$ cm^{-2} for DR 21 and $(1.9 \pm 0.3) \times 10^{14}$ cm^{-2} for DR 21 (OH). Turner and Gammon (1975) have estimated densities of 2.5×10^4 and 6×10^4 cm^{-3}, respectively, for these sources from CN observations. Linke and Goldsmith (1980) obtain 6×10^4 cm^{-3} for both sources from CS observations. However, Wootten, Snell, and Evans (1980) derive a density of 7×10^5 cm^{-3} for DR 21 (OH) from H_2CO. In either case, it seems that CH_3CCH is likely to be excited approximately to LTE so that the true column densities should not differ greatly from the above estimates. The linear dimension of both regions is ~ 1 pc (Dickel, Dickel, and Wilson, 1978) so that the lower density estimate yields H_2 column densities of $\sim 2 \times 10^{23}$ cm^{-2} and a relative CH_3CCH abundance of $\sim 10^{-9}$. To within the rather large uncertainties, this is consistent with the previous results.

e) S 140

The apparent kinetic temperature is 32.1 ± 6.7 K, which agrees with the kinetic temperature of 32 K derived by Blair *et al.* (1978) from CO observations and 32 ± 9 K derived by Ho, Martin, and Barrett (1981) from NH_3 observations.

The model of Blair *et al.* (1978) yields an H_2 density of 8×10^4 cm^{-3} inside a 1′ radius or a column density of $\sim 7 \times 10^{22}$ cm^{-2}. Since the density appears to be high enough to thermalize CH_3CCH, we deduce a relative CH_3CCH abundance of 2.4×10^{-9}, in good agreement with most of the other sources observed.

V. DISCUSSION

The present observations suggest that methyl acetylene is a relatively common molecule in the Galaxy with column densities comparable to those of familiar interstellar molecules such as SO, CS, H_2S (Gottlieb *et al.* 1978; Thaddeus *et al.* 1972) and HC_3N (Avery, MacLeod, and Broten 1982). At our level of sensitivity, it appears that the relative emission from the *K*-components can be adequately modeled assuming local thermodynamic equilibrium and low optical depth. Methyl acetylene may, therefore, be a useful thermometer for the interstellar gas. We note that consistent results were obtained even though the signal-to-noise ratio in the present data is low.

The relative CH_3CCH abundances varies between 1×10^{-9} and 5×10^{-9}. There is some uncertainty as to whether CH_3CCH is thermalized, although the densities derived by various methods for most of these sources suggest that CH_3CCH should be at or near thermal equilibrium. Comparable or possibly greater uncertainty exists in the estimates for total gas column density, with which the CH_3CCH column densities must be compared. Therefore, the present data do not contradict the possibility that CH_3CCH has a fairly uniform relative abundance near 2.5×10^{-9}.

The abundance of CH_3CCH predicted by gas phase calculations is subject to various uncertainties (Huntress and Mitchell 1979). The rate for the reaction $C^+ + H_2 \rightarrow CH_2^+ + h\nu$, which is important in this context, is not measured but inferred from diffuse cloud abundances. The electron abundance is also a crucial parameter. Within the uncertainties, the derived relative abundance of CH_3C_2H is consistent with theory and may serve to constrain the models usefully. The CH_3C_2H abundance is also possibly consistent with certain grain chemistry models (Allen and Robinson 1977), although the model abundance is very dependent on both density and temperature because of surface energetics and depletion effects. Since the observed abundance is predicted in these models only for lifetimes shorter than 10^7 yr, it will be of interest to survey a variety of clouds to see if the abundance varies.

We wish to express special thanks to J. M. Hollis and H. M. Pickett for helpful suggestions. We are grateful to S. Prasad for discussions on interstellar chemical models. The assistance of the NRAO Tucson staff in these observations was invaluable. The research described in this paper was carried out in part at the Jet Propulsion Laboratory, California Institute of Technology, under contract with the National Aeronautics and Space Administration. Partial financial support for B. Zuckerman was provided by National Science Foundation grant AST 76-17600 to the University of Maryland.

REFERENCES

Allen, M., and Robinson, G. W. 1977, *Ap. J.*, **212**, 396.
Avery, L. W., MacLeod, J. M., and Broten, N. W. 1982, *Ap. J.*, **254**, 116.
Bauer, A., Boucher, D., Burie, J., Demaison, J. and Dubrulle, A. 1979, *J. Phys. Chem. Ref. Data*, **8**, 537.
Bevington, P. R. 1969, *Data Reduction and Error Analysis for the Physical Sciences* (New York: McGraw-Hill).
Blair, G. N., Evans, N. J., II, Vanden Bout, P. A., and Peters, W. L., III 1978, *Ap. J.*, **219**, 896.
Cheung, A. C. 1976, Ph.D. thesis, University of California, Berkeley.
Dickel, J. R., Dickel, H. R., and Wilson, W. J. 1978, *Ap. J.*, **223**, 840.
Evans, N. J., II, Zuckerman, B., Sato, T., and Morris, G. 1975, *Ap. J.*, **199**, 383.
Gottlieb, C. A., Gottlieb, E. W., Litvak, M. M., Ball, J. A., and Penfield, H. 1978, *Ap. J.*, **219**, 77.
Harper, D. A. 1974, *Ap. J.*, **192**, 557.
Herzberg, G. 1945, *Infrared and Raman Spectra* (New York: Van Nostrand Reinhold).
Ho, P. T. P., Martin, R. N., and Barrett, A. H. 1981, *Ap. J.*, **246**, 761.
Hollis, J. M., Lovas, F. J., Suenram, R. D., Jewell, P. R., and Snyder, L. E. 1983, *Ap. J.*, **264**, 543.
Hollis, J. M., Snyder, L. E., Blake, P. H., Lovas, F. J., Suenram, R. D., and Ulich, B. L. 1981, *Ap. J.*, **251**, 541.
Huntress, W. T., Jr., and Mitchell, G. F. 1979, *Ap. J.*, **231**, 456.
Linke, R. A., and Goldsmith, P. F. 1980, *Ap. J.*, **235**, 437.
Lovas, F. J., Johnson, D. R., Buhl, D., and Snyder, L. E. 1976, *Ap. J.*, **209**, 770.
Pickett, H. M., and Davis, J. H. 1979, *Ap. J.*, **227**, 446.
Schwartz, P. R., Bologna, J. M., and Waak, J. A. 1978, *Ap. J.*, **226**, 469.
Scoville, N. Z., Solomon, P. M., and Penzias, A. A. 1975, *Ap. J.*, **201**, 352.
Snyder, L. E., and Buhl, D. 1973, *Nature*, **243**, 45.

Snyder, L. E., Hollis, J. M., Lovas, F. J., and Ulich, B. L. 1976, *Ap. J.*, **209**, 67.
Solomon, P. M., Penzias, A. A., Jefferts, K. B., and Wilson, R. W. 1973, *Ap. J. (Letters)*, **185**, L63.
Thaddeus, P., Kutner, M. L., Penzias, A. A., Wilson, R. W., and Jefferts, K. B. 1972, *Ap. J. (Letters)*, **176**, L73.
Turner, B. E., and Gammon, R. H. 1975, *Ap. J.*, **198**, 71.
Turner, B. E., Zuckerman, B., Palmer, P., and Morris, M. 1973, *Ap. J.*, **186**, 123.
Ulich, B. L., and Haas, R. W. 1976, *Ap. J. Suppl.*, **30**, 247.
Wootten, A., Snell, R., and Evans, N. 1980, *Ap. J.*, **240**, 532.

D. F. DICKINSON: Applied Technology, Advanced Systems Division, 645 Almanor Avenue, Sunnyvale, CA 94086

T. B. H. KUIPER: Jet Propulsion Laboratory, T-1166, Pasadena, CA 91109

E. N. RODRIGUEZ KUIPER: Puritan-Bennett Corporation, 12655 Beatrice Street, Los Angeles, CA 90066

B. E. TURNER: National Radio Astronomy Observatory, Edgemont Road, Charlottesville, VA 22901

B. ZUCKERMAN: Astronomy Department, University of California, Los Angeles, CA 90024